

NICMOS IntraPixel Sensitivity

Chun Xu and Bahram Mobasher
September 16, 2003

ABSTRACT

A study of the NICMOS (Camera 3) intrapixel sensitivity is carried out after installation of cryo-cooler in Cycle 11. The consistency of the procedure adopted here is tested by applying it to the data in Cycle 7, as analyzed by Storrs et al (1999), and reproducing their results. The intrapixel sensitivity in Cycle 11 is then measured and compared to that in Cycle 7 (before the installation of the NICMOS cryo-cooler). We find 27% decrease in the intrapixel sensitivity from Cycle 7 to Cycle 11 for both F110W (J-band) and F160W (H-band) filters. The possibility of this effect being due to an increase in the stellar PSF over this period is considered and discarded, as we only find 5% change in the PSF between the two cycles.

1) Introduction

Accurate photometry depends, in part, on the width of the Point Spread Function (PSF) compared to the pixel size. For example, if the PSF is much smaller than the pixel, the detected flux will depend on the position of the PSF on the pixel (i.e. less flux is measured if the PSF is positioned at the corner of a pixel compared to when it covers the entire pixel). This could lead to significant uncertainties in photometric accuracy of sources when the pixel size is larger or comparable to the PSF width.

In case of the NICMOS, this effect is negligible for NIC1 and NIC2, as the PSF core is much broader than their pixel size and hence, to a large extent, the PSF covers the entire pixel. However, NIC3 with a pixel size of 0.2 arcsec, could undersample the PSF at all

wavelengths, leading to different total fluxes for a given star at various dithered positions. Therefore, a correlation is expected between the total light from a given star at different positions on the detector and its corresponding FWHM. This is because, when the PSF is observed towards the edge of a pixel, most of the light is spread over several adjacent pixels, leading to a larger FWHM. On the other hand, when the PSF is centered on a pixel, most of the light is captured by that pixel, leading to a smaller FWHM. In the scenario where most of the light is lost between pixels (which happens when the PSF is too close to the region between pixels where the CdTe layer is prominent), one would expect a relation between FWHM and the amount of light lost. In this study we explore the presence of such relations using the latest dataset from NICMOS.

We aim to quantify the intrapixel sensitivity for NIC3. This follows a similar study of NIC3 pixel sensitivity in Cycle 7 (Storrs et al 1999). To compare the results, a similar procedure is followed and applied on both datasets. The observations are discussed in the next section. We present our method in section 3. Sections 4 and 5 then present measurements of the intrapixel sensitivities in Cycles 11 and 7, with the results compared and discussed in section 6. Correction for intrapixel sensitivity is presented in section 7. We summarize our results in section 8.

2) The Observations

Monitoring of the NICMOS IntraPixel sensitivity was started in Cycle 7 (Storrs et. al. 1999), using Hubble Deep Field South (HDF-S) observations (programs 8058, 8073, 8074, 8087, 8076). These data were taken using NIC3 (SPARS64) with F110W and F160W filters. The observations were also dithered at different positions.

After SM3 and installation of the NICMOS Cryo-cooler in Cycle 11, the study of intrapixel sensitivity was continued with observations of the star cluster NGC1850 (proposal 9638). The observations are done using NIC3 using F110W and F160W filters (STEP256). For each filter a total of 25 exposures of 128 seconds each were obtained. The exposures were dithered by a few pixels, allowing the stellar images to fall at different positions relative to any reference pixel. The data were reduced and calibrated through On-The-Fly reprocessing, using Calnica 4.1.1.

3) The Method

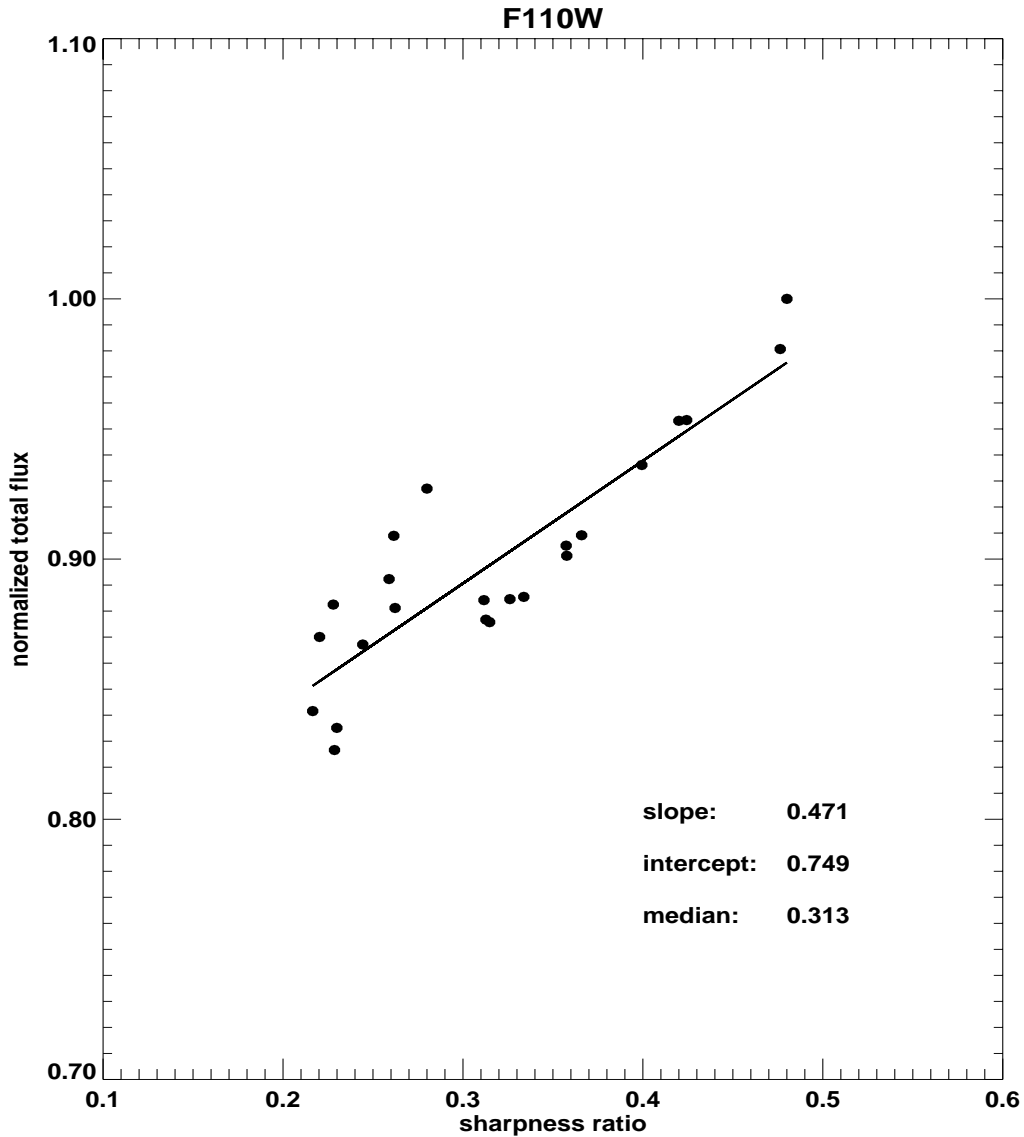
We adopt a variant of the technique used by Storrs et. al. (1999) in Cycle 7. For a given star, we measure the total flux (F_{tot}) within a radius of 2.5 pixels (assuming a FWHM of 1.4 pixels) and the peak flux (F_{pk}) on a single pixel in all dithered exposures of that star. The total flux (F_{tot}) in each exposure is then normalized to the one that has the highest

total flux among all the exposures, i.e., $F_n = \frac{F_{tot}}{\max(F_{tot})}$. The change in the normalized flux (F_n) in a given exposure then reflects the percentage change of the total flux (compared to the reference exposure). We also consider the “sharpness ratio”, S , defined as the ratio of the flux in the peak pixel to that of the total flux (within 2.5 pixel aperture) in the same exposure ($S = \frac{F_{pk}}{F_{tot}}$). This is a measure of the relative subpixel position of a stellar image (or the stellar PSF) with respect to the center of a pixel. For a given star, the closer the stellar image is to the center of a pixel, the more flux that pixel receives, leading to a larger sharpness ratio. We then study the relation between the normalized flux F_n in each exposure and the sharpness ratio S . Ideally, if there are no intrapixel variations, we expect the points on this plot to lie on a horizontal line, i.e., F_n doesn’t change with the relative subpixel positions of the stellar images with respect to any referenced pixel. If there **are** intrapixel variations **and** if the size of the PSF is comparable to or less than that of a pixel, we then expect a trend in the sense that higher sharpness ratios correspond to higher normalized fluxes. The steeper the slope, the higher the intrapixel variations.

4) Measurement of the Intrapixel Sensitivity in Cycle 11

Analysis of the intrapixel sensitivity was carried out within the IDL package. The total stellar and peak pixel fluxes were measured using SExtractor (Bertin & Arnouts 1996). The stars that lie in the crowded regions are excluded from our analysis. Of the stars that are suitable for the analysis, not every exposure was used: if the fitted FWHM of the star was larger than a certain value (we adopted 2.8, corresponding to twice the mean FWHM of the PSF) or if the fitting didn’t converge, as indicated by the “Flag” value in the SExtractor catalogue, then that exposure was excluded. Furthermore, if there were fewer than a certain number (we used 15) of “good” exposures for a selected star, that star was also excluded from our analysis because it might introduce large uncertainties. For the adopted stars and their exposures, the normalized fluxes were plotted against their sharpness ratios. This is presented for a single star in Figure 1, and the linear fit is also shown. Performing this analysis for all the adopted stars, the mean of the slopes is taken and used as a measure of the intrapixel sensitivity. We revisit this later by performing a fit to “all” the stars combined, using a different approach. As our analysis is different in detail from Storrs et al. (1999), to compare the intrapixel sensitivities between Cycle 7 and Cycle 11, we now perform the same analysis on Cycle 7 data so that the results could be directly compared.

Figure 1: The normalized flux vs. sharpness ratio for different exposures of a single star. The linear fit is also shown.



5) Measurement of the IntraPixel Sensitivity in Cycle 7

One aim of this study is to explore changes in intrapixel sensitivity between Cycles 7 and 11. Therefore, exactly the same analysis must be performed on the data taken in the

two Cycles. However, we first compare the results from our analysis of the HDF-S data, taken in Cycle 7 with those of Storrs et al. (1999) on the same dataset.

The Comparison between the two techniques, applied on Cycle 7 HDF-S data compared in the first part of Table 1. This confirms that the two analysis, for both F110W and F160W filters, agree within 3%, implying that the two strategies are consistent. Given this result, we can now directly compare the two analysis carried out on two different fields, in Cycle 7 and Cycle 11.

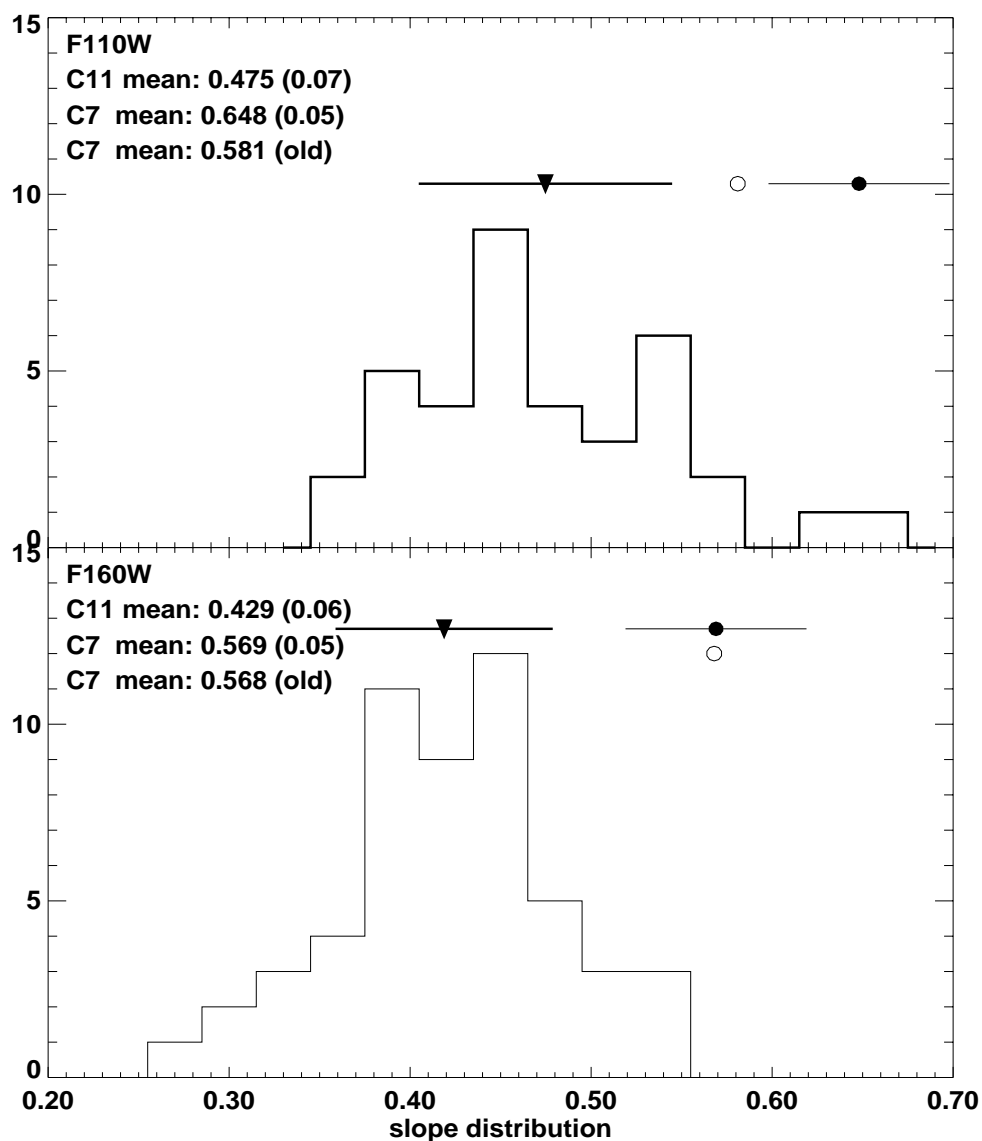
Table 1. The results from Cycle 7 and Cycle 11 data. Results from Storrs et al. (1999) analysis and ours are listed

Data		Filter	Slope	Intercept	Median Sharpness
Cycle 7 (HDF-S)	Storrs et al	F110W	0.581	0.668	0.353
		F160W	0.568	0.706	0.340
	Ours	F110W	0.648 ± 0.05	0.611 ± 0.05	0.386 ± 0.04
		F160W	0.569 ± 0.05	0.683 ± 0.04	0.371 ± 0.01
Cycle 11 (NGC 1850)	Ours	F110W	0.475 ± 0.07	0.753 ± 0.04	0.369 ± 0.04
		F160W	0.419 ± 0.06	0.841 ± 0.02	0.354 ± 0.03

6) Comparison Between Cycle 7 and Cycle 11 Results

The results based on Cycle 11 data (NGC 1850 star cluster) are also listed in Table 1. For both F110W and F160W filters, the average values for the slopes are significantly smaller in Cycle 11 compared to Cycle 7. This is demonstrated in Figure 2 where the distribution of the slopes (corresponding to both F110W and F160W filters) for different stars are presented. In Figure 2 we compare the slopes for Cycle 7 data reduced using the analysis presented here and that in Storrs et al (1999), and between Cycle 7 and Cycle 11 data. This shows that the intrapixel sensitivity has decreased by $\sim 27\%$ from Cycle 7 to Cycle 11 as presented in Table 1. As discussed earlier, slope is a good indicator of the intrapixel sensitivity, and a decrease of the slope reveals either a decrease in intrapixel variation or an increase in the stellar PSF over this period. We will show in the following discussion that the change of slopes is indeed caused by a decrease in the intrapixel sensitivity.

Figure 2: Comparison between NIC3 intrapixel sensitivity results from Cycle 7 and Cycle 11. The histogram and the corresponding measurement, indicated with a filled triangle, are from Cycle 11 data. The filled circle is from our analysis of Cycle 7 data, and the open circle is from Storrs et al. (1999).

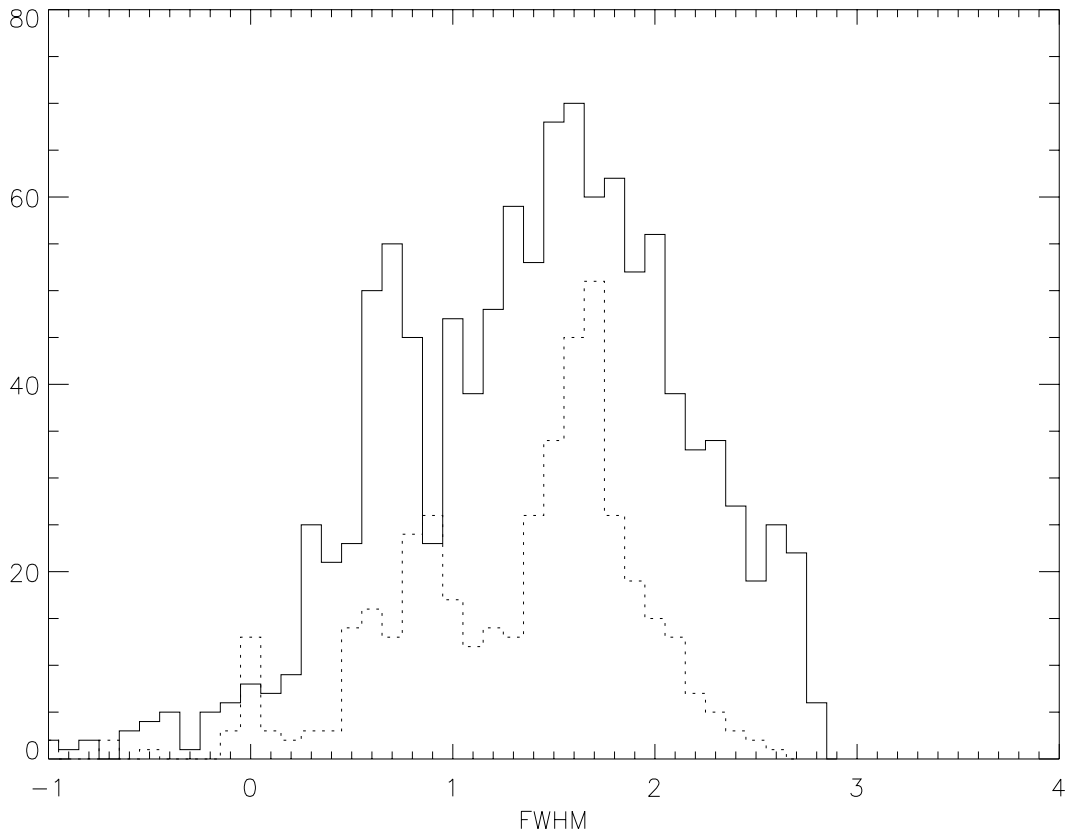


In order to determine whether the change/broadening of the stellar PSF or the intrinsic change of the intrapixel variation lead to the flattening of the slopes from Cycle 7 to Cycle 11, we compare the distribution of the measured FWHM of the stellar PSF from both Cycle 11 and Cycle 7 dataset (Figure 3). The PSF was determined by a gaussian fit to the stellar profile within SExtractor. Only the PSFs from the “good” exposures of each star are

used in making the histogram, corresponding to all the exposures in the slope fitting. It is clear that the stellar PSF does not change between the two datasets. In fact, the measured FWHMs for an ensemble of stars from Cycle 11 data is 1.38 ± 0.70 pixels, compared to 1.30 ± 0.72 pixels from Cycle 7 data. Given this agreement, the change of slope in Figure 2 is interpreted as due to decreases in intrinsic intrapixel sensitivities.

The result in this section is interpreted as follows; The increase in temperature in cycle 11 compared to Cycle 7 leads to an increase of Detector Quantum Efficiency (DQE) for individual pixels, as shown by the flat-field analysis of NICMOS images (Molter, S., et al. 2002, P111). This overall increase in the Does will be relatively higher for pixels with a “lower than average” Does, resulting in less sensitivity to the flatfooted. A similar mechanism could operate in single pixels, leading to less intrapixel variation. Moreover, the increase in temperature also leads to an increase in the electron mobility, which further mimics the increase in DQE within individual pixels.

Figure 3: The histogram of the measured FWHM of the stellar PSF from Cycle 11 data (solid line) and Cycle 7 data (dotted line).



7) The Correction of the IntraPixel Sensitivity

We find that the normalized total flux used above, which was originally defined in Storrs et al (1999), is not the appropriate representation of the total flux of a star. The “maximum” total flux of a star in a series of dithered exposures could be very uncertain, and might be completely different from the “true” flux of that star. The main disadvantage of this definition is that we cannot perform a linear fit (as in Fig. 1) to all the available stars combined. The reason is that the expected “average” of the normalized total fluxes of different exposures” (which is the value to use for calibration), vary from star to star. In other words, if we plot the sharpness ratio as. normalized total flux for different stars as in Fig. 1, we find that different stars follow different loci. For this reason, we redefine the normalized total flux as the ratio of the total flux of one exposure to the median of the total flux of all different exposures, i.e., $\tilde{F}_n = \frac{F_{tot}}{median(F_{tot})}$. This allows all the stars to lie on the same locus

and therefore making it possible to include all the stars in the fit. The result is listed in Table 2. and shown in Figure 4. It is interesting to note that the data of F110W are more scattered than those of F160W, as indicated by the value dex in Table 2 (dex is defined as the square root mean of the square of deviation of individual points in Figure 4 from the mean line). This is consistent with the fact that F110W suffers more from the intrapixel variations than does F160W, as indicated by their different slopes in Figure 4.

Table 2. The Results according to the new approach, i.e., after normalization of the total stellar flux to the ensemble median value.

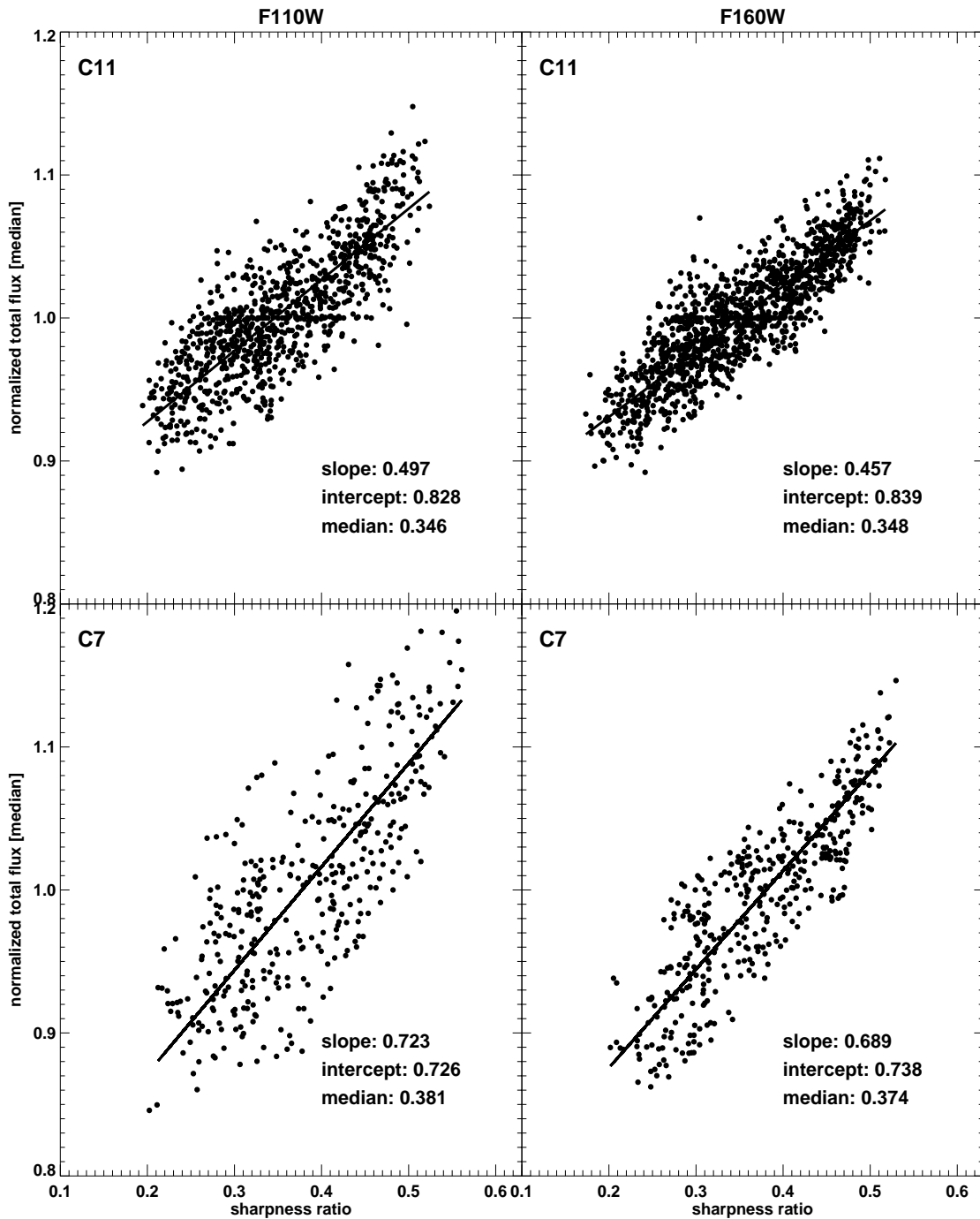
	Filter	Slope (α)	Intercept (β)	Median Sharpness (S)	dex
Cycle 7	F110W	0.689 ± 0.029	0.738 ± 0.011	0.374 ± 0.080	0.025
	F160W	0.723 ± 0.030	0.727 ± 0.012	0.381 ± 0.086	0.038
Cycle 11	F110W	0.497 ± 0.019	0.828 ± 0.007	0.346 ± 0.077	0.023
	F160W	0.457 ± 0.015	0.839 ± 0.005	0.348 ± 0.079	0.019

Using the new definition of the normalized flux, we now derive the relation concerning correction for intrapixel sensitivity. The total flux of an observed star corrected for intrapixel sensitivity (F_c) is: $F_c = F_o \times \frac{\alpha \cdot S + \beta}{\alpha \cdot S_o + \beta}$, where F_o and S_o are respectively the measured flux and sharpness ratio of that star. The parameters α (slope), β (intercept) and

S (median sharpness ratio) are listed in Table 2. The uncertainty of the calibrated flux

(ΔF_c) is given by: $\Delta F_c = F_m \times \frac{dex}{\sqrt{1 + \alpha^2}}$, with the value of dex also listed in Table 2.

Figure 4: The fits to both Cycle 7 and Cycle 11 data using all the stars. The upper two panels correspond to Cycle 11 data while the lower two correspond to Cycle 7 data.



8.) Conclusions

We studied the NICMOS (Camera 3) intrapixel sensitivity in Cycle 11 and compared the results with those from Cycle 7. We found a 27% decrease in the intrapixel sensitivity from Cycle 7 to Cycle 11 for both F110W (J-band) and F160W (H-band) filters. The possibility of this effect being due to an increase in the stellar PSF over this period was considered and discarded, as we only found a 5% change in the PSF between the two cycles. We slightly modified the method of the intrapixel sensitivity correction used by Storrs et al (1999) and updated the coefficient tables accordingly.

We are grateful to Richard Hook and Chris Hanley for helpful discussions on Cycle 7 data. We thank Mark Dickenson for helpful comments and Al Schultz for carefully reading the manuscript.

References

- Bertin, E., and Arnouts, S., 1996, *A&AS*, 117, 393
Storrs, R., Hook, R., Stiavelli, M., Hanley, C., and Freudling, W., 1999, *ISR NICMOS-99-005*
Malhotra, S., et al. 2002, "NICMOS Instrument Handbook", Version 5.0, (Baltimore: STScI).